Proteomic analysis of radioiodine-refractory differentiated thyroid cancer identifies CHI3L1 upregulation in association with dysfunction of the sodium-iodine symporter

YUNJIE LI[1], FENGQIONG HU[2], JIE DENG[3], XIN HUANG[2], CHUNYAN ZHOU[4], MENGXUE WU[5] and DONG DUAN[4]

[1]Department of Nuclear Medicine, The Second People's Hospital of Shenzhen, Shenzhen, Guangdong 518035; [2]Department of Nuclear Medicine, The First Affiliated Hospital of Chongqing Medical University, Chongqing 400016; [3]Department of Nuclear Medicine, The Second Affiliated Hospital of Army Medical University, Chongqing 400037; [4]Department of Nuclear Medicine, Chongqing General Hospital, Chongqing 401147; [5]Department of Nuclear Medicine, The First Hospital Affiliated to Army Medical University, Chongqing 400038, P.R. China

Received July 3, 2022; Accepted November 14, 2022

DOI: 10.3892/ol.2022.13622

Abstract. Radioiodine refractory differentiated thyroid cancer (RR-DTC) is the main factor adversely affecting the overall survival rate of patients with thyroid cancer. The aim of the present study was to investigate the underlying molecular mechanism of pathogenesis of RR-DTC and to explore novel therapeutic targets for clinical treatment. A proteomic analysis was performed using the tumor tissues of patients with RR-DTC. A total of 6 metastatic lymph nodes were collected during lymph node dissection, 3 from patients with RR-DTC and 3 from patients with papillary thyroid cancer. The expression of chitinase-3-like 1 (CHI3L1) and sodium-iodine symporter (NIS) in the tumor tissue was detected by immunohistochemistry (IHC). Western blotting was used to detect the expression of CHI3L1, phosphorylated (p)-MEK and p-ERK1/2 in PTC-K1 cells transfected with CHI3L1 overexpression vector. The proteomic analysis identified 665 differentially expressed proteins (DEPs), including 327 upregulated and 338 downregulated proteins in the RR-DTC group, which were enriched in 59 signaling pathways by Kyoto Encyclopedia of Genes and Genomes database analysis. In particular, CHI3L1 was demonstrated to be significantly upregulated in RR-DTC as evidenced by quantitative proteomic analysis and IHC. Western blotting suggested that the overexpression of CHI3L1 activated the MEK/ERK1/2 signaling pathway, which may lead to NIS dysfunction. In conclusion, the present study suggests that CHI3L1 is a potential molecular target for the radiotherapy of patients with RR-DTC.

Correspondence to: Dr Dong Duan, Department of Nuclear Medicine, Chongqing General Hospital, 118 Xingguang Avenue, Yubei, Chongqing 401147, P.R. China
E-mail: duandong26@163.com

Abbreviations: RR-DTC, radioiodine-refractory differentiated thyroid cancer; CHI3L1, chitinase-3-like 1; NIS, sodium-iodine symporter; IHC, immunohistochemistry; DEPs, differentially expressed proteins; DTC, differentiated thyroid cancer; PTC, papillary thyroid cancer; GO, Gene Ontology; KEGG, Kyoto Encyclopedia of Genes and Genomes; MS, mass spectrometry; FFPET, formalin-fixed paraffin-embedded tissue; ECM1, extracellular matrix protein 1; CDC42, cell division control protein 42; RAC2, Ras-related C3 botulinum toxin substrate; ALDH, aldehyde dehydrogenase; CD44, cluster of differentiation 44; p-, phosphorylated

Key words: comparative proteomics, radioiodine-refractory thyroid cancer, chitinase-3-like 1, sodium-iodine symporter, targeting therapy

Introduction

The incidence of thyroid cancer is reported to have increased at an annual rate of 3.6% between 1974 and 2013 in the USA (1,2). Patients with differentiated thyroid cancer (DTC), including papillary thyroid cancer (PTC) and follicular thyroid cancer, usually have a favorable prognosis due to the good efficacy of conventional treatments, particularly postoperative radiotherapy (3), which plays an important role in eradicating any residual tumor and targeting distant metastases (4). When patients with DTC begin to resist the uptake of radioiodine during radiotherapy, radioiodine-refractory DTC (RR-DTC) develops, which occurs in 15-20% cases of thyroid cancer (5). Patients with RR-DTC usually have a poor prognosis due to their impaired radioiodine uptake; it has been reported that patients with RR-DTC have a median survival time of only 3-6 years once diagnosed (6). The pathology of radioiodine resistance may be associated with tumor cell dedifferentiation, which greatly increases malignancy (7,8). It would be of great benefit to explore the exact underlying molecular mechanism of tumor cell dedifferentiation and iodine resistance in order to improve the survival rate of patients with RR-DTC.

Generally, patients with DTC have a favorable prognosis. Traditional radiotherapy can effectively remove tumor tissue remaining following thyroidectomy and any distant metastases

via the action of beta-rays emitted during radioiodine decay (9). However, the typical pathophysiological feature of RR-DTC is the reduced or deficient capacity for iodine uptake, which results in the lack of efficacy of iodine-dependent regimens in its treatment. However, it has been reported that when artificially engineered to bind to tumor targets, radiopharmaceuticals are able to eliminate tumor cells in a similar manner to radioiodine (10,11). Considering the advantages of radiotherapy in the clinical treatment of DTC, the present study aimed to identify a potential molecular target to which radiopharmaceuticals could be directed for the radiotherapy of RR-DTC.

The process of iodine accumulation depends on the sodium iodine symporter (NIS), a protein complex in the plasma membrane of thyroid epithelial cells (12). Studies have shown that in RR-DTC, low expression levels of NIS pose a great challenge to the eradication of residual tumor and distant metastases, which can lead to the spread of the tumor (13). Therefore, the expression level of NIS is responsible for iodine uptake capacity to a certain extent and its relationship with the pathogenesis of RR-DTC requires further exploration.

Owing to the high-throughput and stability of proteomic technology, it is widely used in cancer research to identify differentially expressed proteins (DEPs) for diagnostic and therapeutic purposes. Gene Ontology (GO) and Kyoto Encyclopedia of Genes and Genomes (KEGG) databases can be used to cluster these identified DEPs in order to screen for potential biomarkers and dynamically monitor the progression of diseases. On this basis, previous studies have revealed that activation of the MAPK and PI3K signaling pathways are closely associated with tumorigenesis since they change the cellular microenvironment, promote tumor neovascularization and stimulate tumor cell proliferation (14,15). In addition, the MAPK/ERK signaling pathway has been found to have regulatory effect on cell differentiation in studies of breast cancer and rhabdomyosarcoma, which could potentially be the mechanism underlying the dedifferentiation of tumor cells in RR-DTC (16,17). However, investigations of the specific DEPs and signaling pathways associated with RR-DTC are lacking, and were therefore performed in the present study.

To the best of our knowledge, the present study is the first to perform a proteomic analysis of the tumor tissue of patients with RR-DTC. Tumor tissue from patients with PTC, the most common type of DTC, was employed as a control. Isobaric tags for relative and absolute quantification (iTRAQ) technology was used to identify the DEPs. Further functional analysis of DEPs was performed with the use of GO and KEGG databases. Proteins of interest were verified by immunohistochemistry (IHC) and western blotting.

Materials and methods

Sample collection. Inclusion criteria for sample collection of RR-DTC were as follows: i) Patients who had undergone a total thyroidectomy, with lesions confirmed as PTC pathologically; ii) patients who had undergone >3 cycles of radioiodine therapy, with metastasis confirmed as not avid for radioiodine on the last whole-body scan (WBS); and iii) the concentration of thyroglobulin increased every 3 months during the long-term follow-up. In accordance with the inclusion criteria, 3 metastatic lymph nodes from 3 patients with RR-DTC and 3 metastatic lymph nodes from 3 patients with PTC were collected. Samples were collected from the First Affiliated Hospital of Chongqing Medical University (Chongqing, China) between August 2019 and September 2020. The exclusion criteria were as follows: i) Patients whose lesion was avid for radioiodine at any rate despite receiving >600 mCi radioiodine in total; ii) patients who had ever taken targeted drugs such as sorafinib or lentatinib; iii) patients with multiple distant metastases or who were in a poor condition; and iv) patients whose lesions were not avid for radioiodine but were in a stable condition. All lymph nodes were rinsed with PBS three times, after which each lymph node was incised to provide two parts, one of which was used to prepare formalin-fixed paraffin-embedded tissue (FFPET) for IHC while the other was stored at -80˚C for proteomic analysis. In addition, to enlarge the sample size, a further 6 metastatic lymph nodes from patients with PTC and RR-DTC (3 of each) were included in addition to those from the aforementioned patients. These samples were collected from the Department of Pathology of the First Affiliated Hospital of Chongqing Medical University between April 2019 and January 2020. The study was approved by Chongqing Medical University Ethics Committee and all patients involved provided written informed consent to participate.

Proteomics technology and bioinformatics analysis. All samples were subjected to proteomic analysis using iTRAQ technology coupled with mass spectrometry (MS) according to the manufacturer's protocol. For MS, polarity was set in a positive ion mode and data-dependent manner, with full MS scans from 350 to 2,000 m/z, full scan resolution set at 70,000, ion source voltage set at 1.8 eV and MS/MS scan resolution set at 17,500. The raw MS data were loaded into Proteome Discoverer (PD) 1.4 (Thermo Fisher Scientific, Inc.), which selected mass spectra using preset criteria as follows: Mass range of parent ion, 350 to 6,000 Da; S/N, 1.5. The selected mass spectra were searched using Mascot (version 2.3.0; Matrix Science) to identify proteins. After that, the PD software was used to perform a quantitative analysis based on the search results and selected mass spectra. In the proteomic analysis, a fold change >1.2 was regarded to indicate a DEP between two groups according to previous studies (18-20). According to the outcome of the quantitative analysis, all identified DEPs were subjected to functional annotation using the GO (http://geneontology.org/) and KEGG databases (https://www.kegg.jp).

IHC. FFPET sections for the IHC assay were provided by the Department of Pathology of the First Affiliated Hospital of Chongqing Medical University. The thickness of each section was 5 μm. For antigen retrieval, all sections were heated by water bath at 95˚C with 0.01 mol/l sodium citrate buffer for 20 min, and then cooled to room temperature and washed with PBS 3 times. The expression of NIS and CHI3L1 was examined following quenching of endogenous peroxidase activity and blocking the sections using an immunohistochemical kit at room temperature for 15 min (cat. no. SP9000; Beijing Zhongshan Golden Bridge Biotechnology Co., Ltd.). Antibodies targeting NIS (bs-0048R; Bioss) and CHI3L1 (ab77528; Abcam) were diluted to optimal concentrations

(1:300 and 1:1,000, respectively). The primary antibodies were incubated at 4˚C overnight. All sections were incubated for 30 min at 37˚C after addition of the secondary antibody, which was diluted by PBS at 1:100 (part of kit; cat. no. SP9000; Beijing Zhongshan Golden Bridge Biotechnology Co., Ltd.). Each section was observed under a microscope after being processed with DAB solution, counterstaining with hematoxylin at room temperature for 30 sec, dehydration, and transparentization using ethanol and xylene. ImageJ software (version 1.53; National Institutes of Health) was used to evaluate the immunostaining intensity.

Cell culture and lentiviral transfection. PTC-K1 cells were purchased from Otwo Biotech. The PTC-K1 cells were authenticated by STR profiling; they are considered as a subpopulation of the Glag-66 cell line, and both cell lines are papillary thyroid carcinoma cells. The cells were cultured in complete DMEM, comprising 89% DMEM supplemented with 10% FBS and 1% penicillin-streptomycin by volume, and maintained in an incubator with 5% carbon dioxide at 37.0˚C and 95% humidity. A CHI3L1 overexpression lentiviral vector (PSE3748; 2nd generation) and control vector (PMT222; 2nd generation), obtained from SANGON Biotech, were used to infect PTC-K1 cells following the manufacturer's protocol. pLvx-AcGEP (3 μg) was used for transfection and the ratio of pLvx-AcGFP, psPAX and pMD2.G was set at 4:3:1. Cells were transfected at 37˚C for 48 h. The multiplicity of infection was set at 30. Cells were cultured in 2 μg/ml puromycin for 2 weeks until the CHI3L1 overexpression and control transfection were stable.

Western blotting. Total protein was extracted from the cells using RIPA buffer (P0013B; Beyotime Institute of Biotechnology) containing protease inhibitor (100:1 by volume). The concentration of total protein was then measured using a BCA protein assay kit. A sample containing 40 μg protein per lane was loaded onto a 10% SDS-PAGE gel (P0012A; Beyotime Institute of Biotechnology). Proteins were transferred to a PVDF membrane and blocked using 5% BSA blocking buffer (cat. no. SW3015; Beijing Solarbio Science & Technology Co., Ltd.) for 2 h at room temperature. Antibodies targeting CHI3L1, phosphorylated MEK1 (p-MEK1; cat. no. ab96379; Abcam), phosphorylated ERK1/2 (p-ERK1/2; cat. no. ab201015; Abcam) and GAPDH (AB-P-R001; Hangzhou Goodhere Biotechnology Co., Ltd.) were used at dilutions of 1:1,000, 1:500, 1:1,000, and 1:500, respectively. The primary antibodies were incubated at 4˚C overnight, and the secondary antibody diluted at 1:2,000 (cat. no. A0279; Beyotime Institute of Biotechnology) was incubated at 37˚C for 1 h. Visualization reagent (cat. no. P0018S; BeyoECL plus) was obtained from Beyotime Institute of Biotechnology. ImageJ software (version 1.53) was used to measure the band density for quantitative analysis.

Statistical analysis. Statistical analysis was performed using Student's unpaired t-test or one-way analysis of variance followed by Tukey's multiple comparisons test for post hoc testing. SPSS 22.0 (IBM Corp.) and GraphPad Prism 7.00 (GraphPad Software, Inc.) software were used to perform the analyses. All data are presented as the mean ± SD. $P<0.05$ was considered to indicate a statistically significant difference.

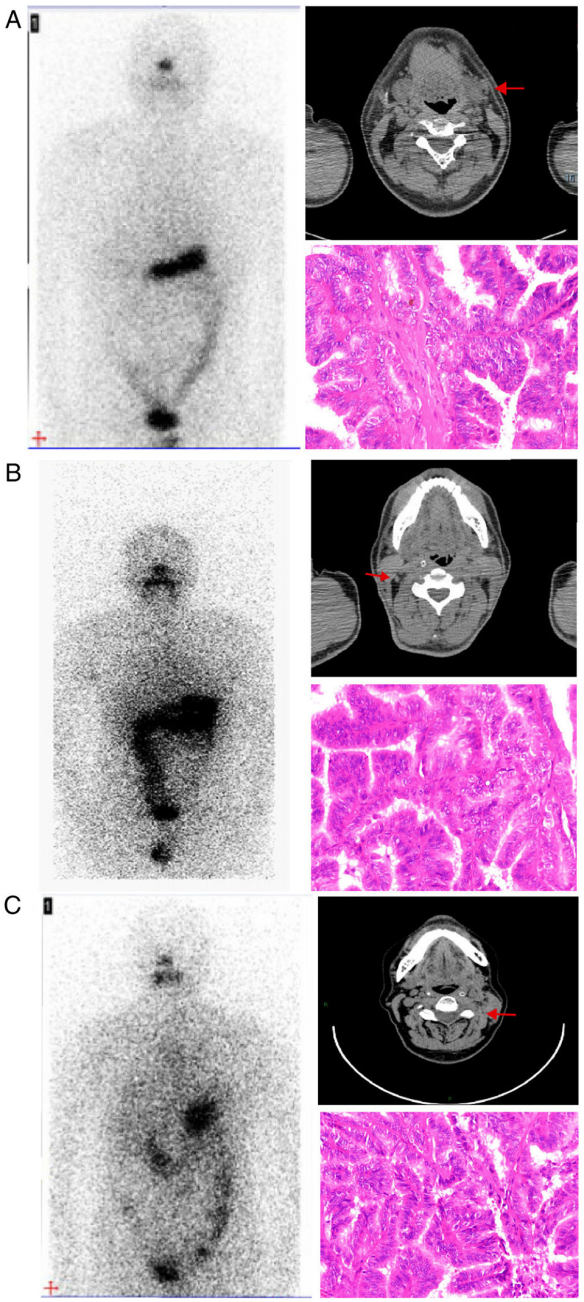

Figure 1. Imaging characteristics and pathological sections of three patients with RR-DTC who were subjected to proteomic analysis. (A) Patient 1, a 31-year-old male. One metastatic lymph node was detected on the left side of the neck (red arrow) by CT imaging (upper right panel) while no abnormal radioactive 131-iodine uptake was observed by WBS (left panel). (B) Patient 2, a 49-year-old male. One metastatic lymph node was found on the right side of the neck (red arrow) by CT imaging (upper right panel) while no abnormal radioactive 131-iodine uptake was observed by WBS (left panel). (C) Patient 3, a 52-year-old female. One metastatic lymph node was found on the left side of the neck (red arrow) by CT imaging (upper right panel) while no abnormal radioactive 131-iodine uptake was observed by WBS (left panel). All the lymph nodes obtained from the three patients were verified to be papillary thyroid cancer by pathological sections (x400 magnification; lower right panels). CT, computed tomography; WBS, whole-body scan.

Results

Clinical characteristics of patients included for proteomic analysis. All patients with RR-DTC involved were eligible for inclusion based on a radioiodine WBS and pathological

Table I. Clinical characteristics of the patients for proteomic analysis.

Characteristics	RR-DTC			PTC		
Sex	Male	Male	Female	Male	Male	Female
Age (years)	31	49	52	38	29	35
TNM stage	$T_2N_{1b}M_0$	$T_2N_{1b}M_0$	$T_1N_{1b}M_0$	$T_1N_{1b}M_0$	$T_1N_{1b}M_0$	$T_1N_{1b}M_0$
^{131}I therapies (n)	4	5	2	2	2	2
Pathological type	PTC	PTC	PTC	PTC	PTC	PTC
BRAF mutation	-	+	+	-	+	+

RR-DTC, radioiodine-refractory differentiated thyroid cancer; PTC, papillary thyroid cancer.

sections. Computed tomography imaging demonstrated the presence of metastatic lymph nodes in cervical locations, while no abnormal radioiodine uptake was detected in the corresponding locations according to the WBS. Following cervical lymph node dissection, the metastatic lymph nodes were identified to be PTC by inspection of the pathological sections (Fig. 1). The clinical characteristics of the patients included in the proteomic analysis are shown in Table I.

BRAF mutation is not closely associated with NIS expression. To investigate whether BRAF mutation inhibits NIS expression in RR-DTC, the immunohistochemical analysis of NIS was performed in 24 FFPET sections collected from different patients, including PTC BRAF (+) tissues, PTC BRAF (-) tissues, RR-DTC BRAF (+) tissues, and RR-DTC BRAF (-) tissues (6 sections/group). As shown in Fig. 2, no significant difference was detected among the four groups with regard to the positive rate of NIS expression.

DEPs between RR-DTC and PTC. The proteomic analysis detected 665 DEPs between the RR-DTC and PTC groups. A total of 327 proteins were upregulated in RR-DTC compared with PTC, including CHI3L1, extracellular matrix protein 1 (ECM1), 14-3-3 ε and 14-3-3 σ, while 338 proteins were downregulated, including myosin-9, cell division control protein 42 (CDC42) and Ras-related C3 botulinum toxin substrate (RAC2). Notably, cancer stem cell markers including aldehyde dehydrogenase (ALDH) and cluster of differentiation 44 (CD44) were found to be upregulated in RR-DTC compared with DTC. GO functional annotation demonstrated that DEPs were enriched in 'biological process', 'cellular process', 'biological regulation', 'regulation of biological process', 'regulation of cellular process' and 'response to stimulus' (Fig. 3). KEGG analysis revealed that the DEPs were enriched in 59 signaling pathways, which included 'valine, leucine and isoleucine degradation', 'beta-alanine metabolism', 'focal adhesion', 'carbon metabolism' and 'fatty acid degradation' (Fig. 4).

CHI3L1 is significantly upregulated in RR-DTC compared with PTC and activates the MEK/ERK1/2 signaling pathway. CHI3L1 expression was approximately twice as high in RR-DTC than in DTC according to the results of the proteomic analysis. For the purpose of enlarging the sample size and verifying the reliability of the proteomic results, IHC for CHI3L1 was performed on 12 FFPET sections collected from 6 patients with RR-DTC and 6 patients with PTC. The clinical characteristics of the patients included for IHC are shown in Table II. Consistent with the results of the proteomic analysis, CHI3L1 expression was significantly stronger in RR-DTC than in PTC. In addition, CHI3L1 was observed to be located in the cytoplasm and membrane by IHC (Fig. 5).

Finally, as shown in Fig. 6, PTC-K1 cells were successfully transfected with CHI3L1 overexpression vector. The levels of p-MEK1 and p-ERK1/2 were higher in the cells stably transfected with CHI3L1 overexpression vector than in those stably transfected with the empty vector and the untransfected PTC-K1 control. No marked difference in the levels of p-MEK1 and p-ERK1/2 were detected between the empty vector and untransfected control.

Discussion

In the present study, proteomic analysis was performed in patients with RR-DTC to investigate the DEPs associated with the pathogenesis of RR-DTC and screen them for a potential therapeutic target. The results revealed 327 upregulated and 338 downregulated DEPs that were mainly enriched in 59 signaling pathways in RR-DTC. Among these DEPs, CHI3L1 was verified to be significantly upregulated and its transmembrane structure may indicate that this protein is a potential therapeutic target for radiotherapy in patients with RR-DTC.

Notably, the tumor tissue collected for the RR-DTC group in this study was all from patients with PTC. Therefore, PTC tissue was selected as the control group for the proteomic analysis of RR-DTC, while most tumor studies select normal tissues adjacent to tumors as the control (21,22). The DEPs obtained in the present study may provide an improved reflection of the discrepancy between tumor cells of the same pathological type and with different degrees of differentiation. Markers for cell dedifferentiation, including ALDH and CD44 were found to be overexpressed in RR-DTC, which is consistent with previous literature (23-25).

NIS is considered to be strongly associated with radioiodine uptake in thyroid cancer (26). However, no significant difference was detected in the NIS expression level between the RR-DTC and PTC groups in the present study. Notably, numerous DEPs were found to be enriched in biological processes associated with NIS, including 'ion transport' (GO:0006811), 'sodium ion transport' (GO:0006814) and

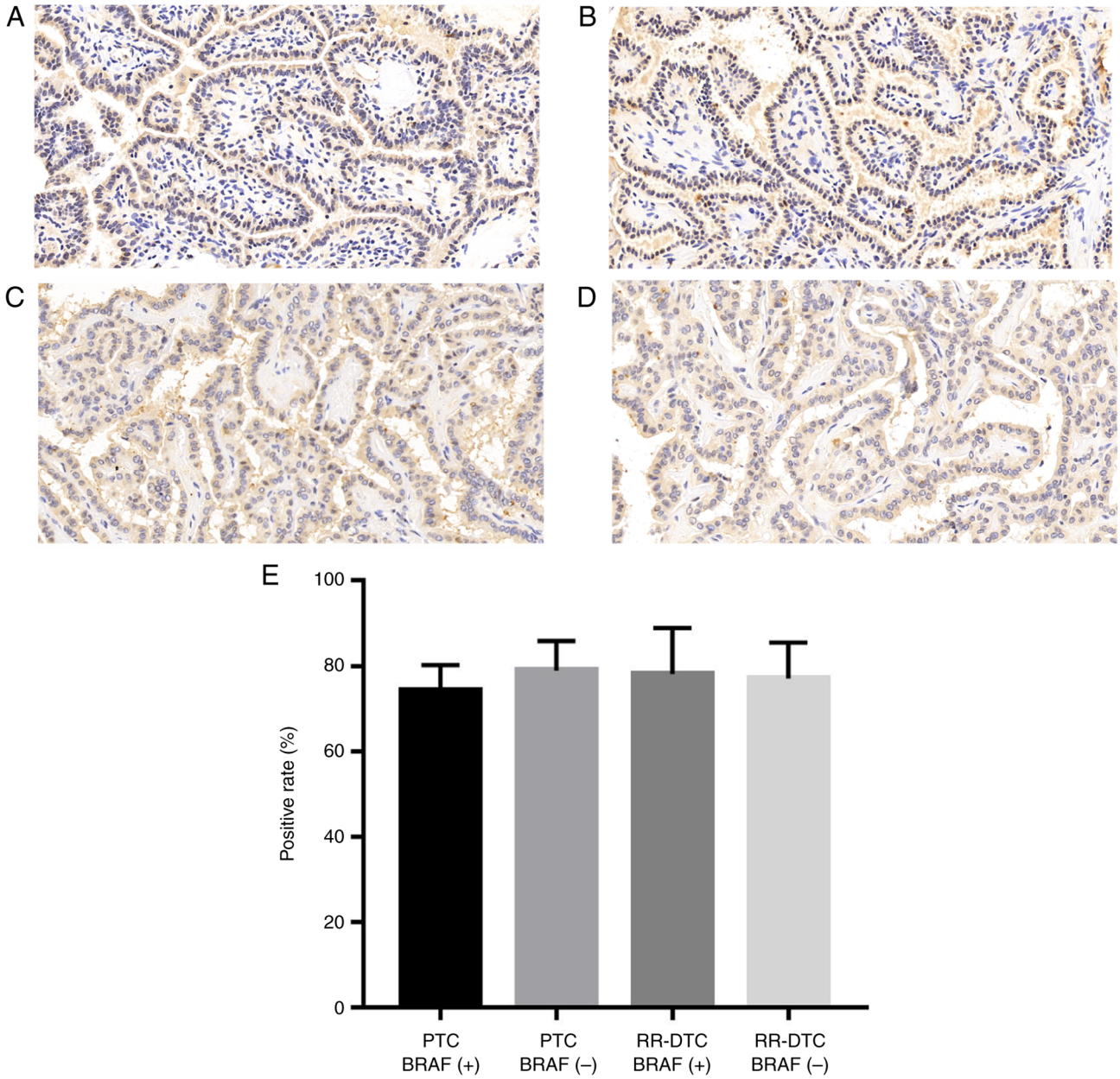

Figure 2. Immunohistochemical staining of NIS in PTC and RR-DTC tissues. (A) PTC BRAF (+) tissue, (B) PTC BRAF (-) tissue, (C) RR-DTC BRAF (+) tissue and (D) RR-DTC BRAF (-) tissue. (E) Statistical analysis of the positive staining rate in the four groups: No significant difference was detected among the four groups. NIS, sodium-iodine symporter; PTC, papillary thyroid cancer; RR-DTC, radioiodine refractory differentiated thyroid cancer.

'transmembrane transport' (GO:0007571), suggesting that even though the total amount of NIS was not reduced, the NIS may be in a non-functional state. The low expression of some trans-membrane transport-associated proteins detected in RR-DTC, including 14-3-3 η, mitochondrial ATP synthase subunit-E and receptor tyrosine protein phosphatase, may also be associated with NIS dysfunction. However, the specific mechanism requires further investigation.

Numerous DEPs were identified in the proteomic analysis, including ECM1, glutathione S-transferase, RAC2, CDC42, myosin regulatory light polypeptide 9 and actinin. These proteins are able to regulate tumor angiogenesis, invasion, metastasis and cell dedifferentiation (27,28), whereby they may potentially modulate the progression of RR-DTC. For example, RAC2 and CDC42 were found to be significantly downregulated in RR-DTC. We hypothesize that these proteins are positively associated with cell differentiation via the promotion of the expression of c-Jun N-terminal kinase 2. This may be one of the molecular mechanisms underlying the poor differentiation of RR-DTC.

Previous studies have demonstrated that CHI3L1 is highly expressed in PTC compared with adjacent normal tissues (29,30), and it was further identified that CHI3L1 is significantly upregulated in RR-DTC compared with PTC in the present study. These findings suggest that CHI3L1 may serve an important role in thyroid cancer and could be associated with the dedifferentiation of tumor cells in RR-DTC. Furthermore, p-MEK1 and p-ERK1/2 levels were markedly higher in stably CHI3L1 overexpressing PTC-K1 cells compared with empty vector transfected controls, indicating

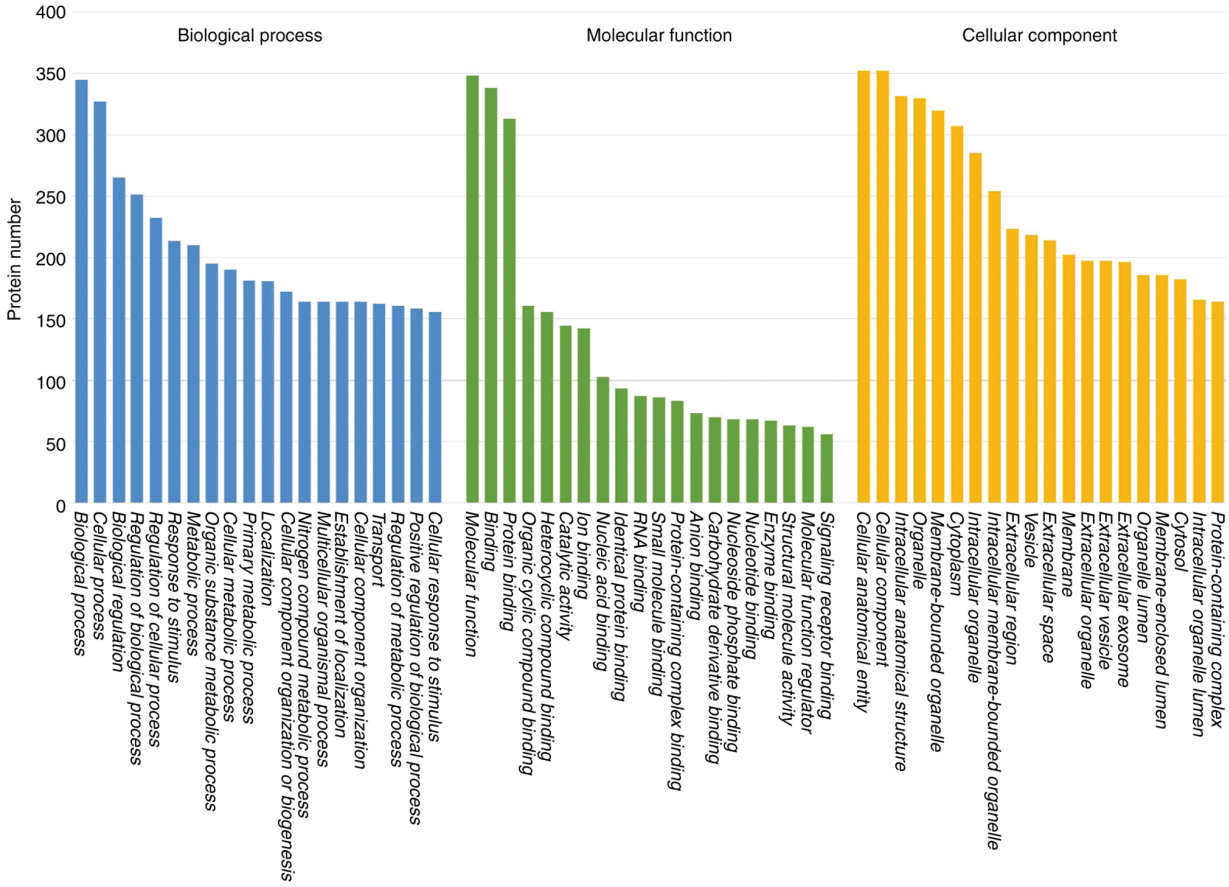

Figure 3. Gene Ontology functional annotation of differentially expressed proteins between patients with radioiodine refractory differentiated thyroid cancer and papillary thyroid cancer.

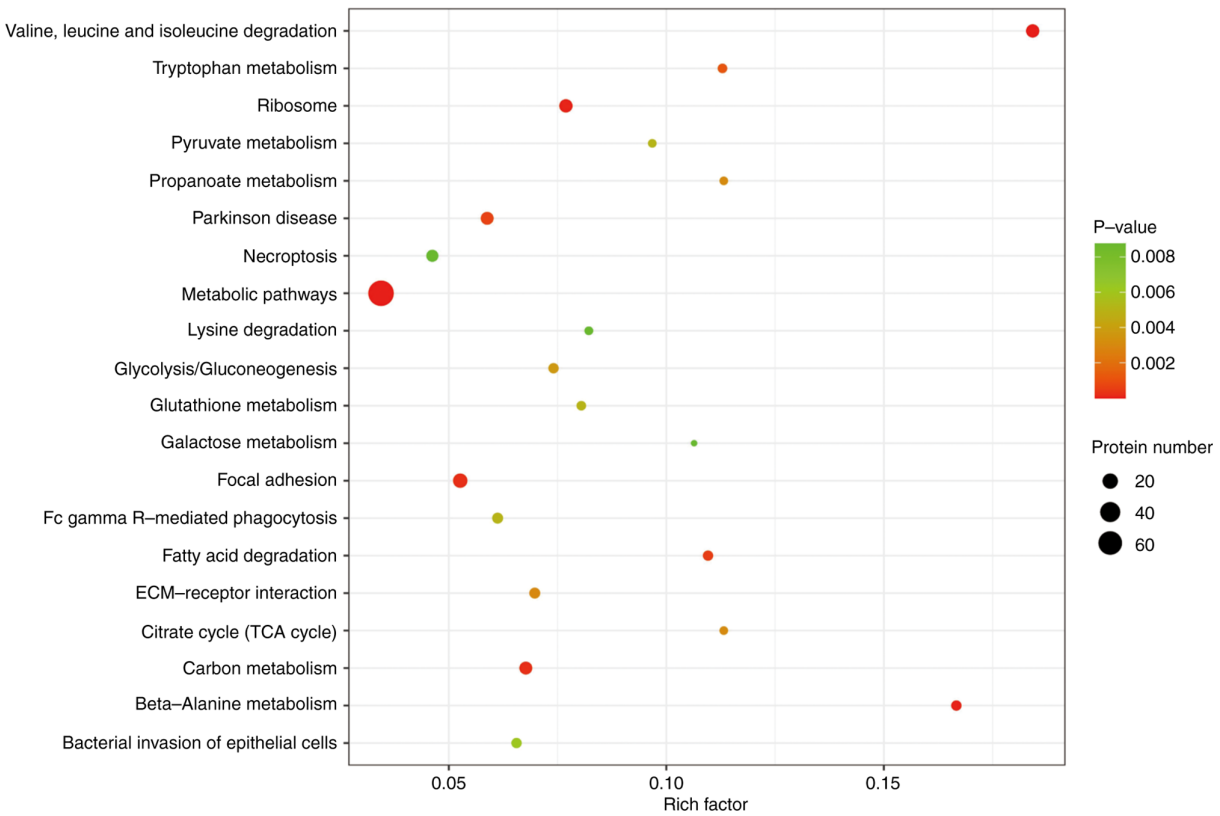

Figure 4. Kyoto Encyclopedia of Genes and Genomes pathway analysis of differentially expressed proteins between patients with radioiodine refractory differentiated thyroid cancer and papillary thyroid cancer.

Table II. Clinical characteristics of patients for IHC of CHI3L1.

Characteristics	RR-DTC			PTC		
Sex	Male	Male	Male	Male	Female	Female
Age (years)	45	56	34	27	38	42
TNM stage	$T_1N_{1b}M_0$	$T_2N_{1b}M_0$	$T_1N_{1b}M_0$	$T_1N_{1a}M_0$	$T_1N_{1b}M_0$	$T_1N_{1b}M_0$
^{131}I therapies (n)	4	3	5	2	2	2
Pathological type	PTC	PTC	PTC	PTC	PTC	PTC
BRAF mutation	-	+	+	+	-	-

RR-DTC, radioiodine-refractory differentiated thyroid cancer; PTC, papillary thyroid cancer; IHC, immunohistochemistry; CHI3L1, chitinase-3-like 1.

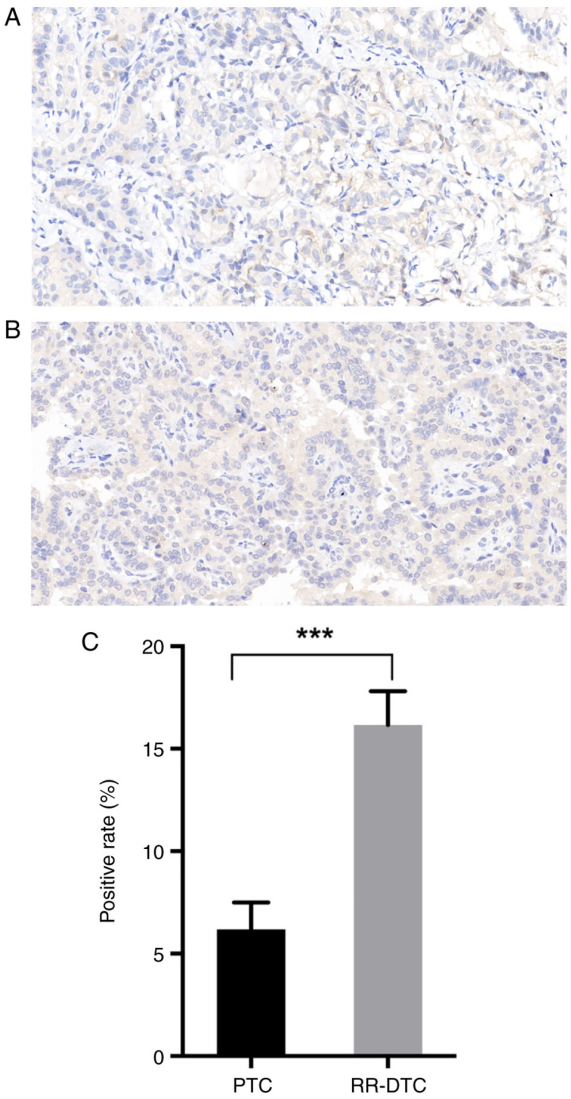

Figure 5. Immunohistochemical staining of CHI3L in PTC and RR-DTC tissue. Representative (A) PTC and (B) RR-DTC staining images. (C) Quantitative analysis of the positive rate of CHI3L. ***P<0.001 for RR-DTC vs. PTC. CHI3L, chitinase-3-like 1; PTC, papillary thyroid cancer; RR-DTC, radioiodine refractory differentiated thyroid cancer.

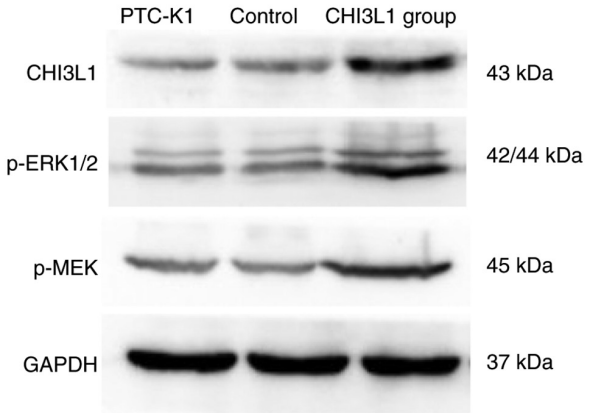

Figure 6. Western blotting of CHI3L, p-MEK and p-ERK1/2 proteins in different grouups. The expression of CHI3L was successfully increased by transfection with CHI3L1 overexpression vector. The protein levels of p-MEK and p-ERK1/2 in the CHI3L1 overexpression group were upregulated compared with those in the PTC-K1 and control groups, which suggested that CHI3L1 overexpression induced activation of the MEK/ERK1/2 signaling pathway. PTC-K1, untransfected cells; control, cells transfected with empty vector; CHI3L1 group, CHI3L1 overexpressing cells. CHI3L1, chitinase-3-like 1; p-, phosphorylated.

activation of the MEK/ERK1/2 signaling pathway in RR-DTC. KEGG analysis suggests that activation of the MAPK/ERK signaling pathway leads to poor cell differentiation in tumor tissues, which is basically consistent with the results of the present study. Therefore, we hypothesize that CHI3L1 leads to poor cell differentiation via activation of the MEK/ERK1/2 signaling pathway in RR-DTC, and the upregulation of CHI3L1 in RR-DTC might explain the poor prognosis of RR-DTC compared with PTC.

Ideally, all the identified DEPs should be screened to identify whether they meet the criteria of a radiotherapeutic target. An eligible target would be upregulated in RR-DTC to bind with its specific probe. Also, probe-receptor combination is favored when the target protein is located on the membrane surface and has a transmembrane structure. Using the protein structure homology-modeling server SWISS-MODEL (https://swissmodel.expasy.org/), the structure of CHI3L1 (accession no. P36222) makes it a suitable radiotherapy target. With seven transmembrane domains, CHI3L1 has the same properties as the NIS. The transmembrane domains ensure that CHI3L1 adheres well to the membrane and its membrane location readily allows the binding of a specific polypeptide or antibody. The IHC results in the present study revealed that CHI3L1 is located in the cytoplasm and membrane, which

is consistent with the predicted structure. Furthermore, the upregulation of CHI3L1 in RR-DTC may allow engagement with a specific polypeptide or antibody around the lesion, thereby reducing radiation damage to normal tissue. In a previous study on osteosarcoma, a specific ligand for CHI3L1 was successfully designed, prepared and verified to inhibit cell migration and invasion (31). Therefore, we hypothesize that a novel agent combining a radionuclide-labeled specific polypeptide or antibody targeting CHI3L1 has the potential to achieve targeted radiotherapy for RR-DTC, which may improve the poor prognosis of patients and alleviate their anxiety.

The present study has certain limitations. Most cases of RR-DTC lose the opportunity to undergo surgery because of distant metastases, which creates a major barrier to sample collection. Therefore, the identified DEPs were not extensive enough to fully elucidate the pathogenesis of RR-DTC due to the small sample size and individual heterogeneity. In addition, the number of screened DEPs was so large that it was not possible to process and analyze them all, and so other potential therapeutic targets for RR-DTC may have been missed. Also, it should be noted that only the PTC-K1 cell line was included in the *in vitro* assays; the inclusion of more PTC cell lines might improve the reliability of the study. Furthermore, the total amounts of MEK and ERK1/2 were not detected by western blotting, so the ratio of phosphorylated protein/total protein could not be determined and the activation level of this signaling pathway could not be evaluated properly.

In conclusion, the present study is the first to obtain the DEPs between PTC and RR-DTC. These DEPs may provide an improved perspective for analysis of the pathogenesis of RR-DTC. In addition, it revealed that significantly upregulated CHI3L1 may be responsible for the poor cell differentiation in RR-DTC and could be an appropriate target for radiotherapy in the future.

Acknowledgements

Not applicable.

Funding

The study was financially supported by the General Program of Natural Science Foundation of Chongqing (cstc2019jcyj-msxmX0327).

Availability of data and materials

The datasets used and/or analyzed during the current study are available from the corresponding author on reasonable request. The proteomics datasets generated and/or analyzed during the present study are available in the ProteomeXchange (http://proteomecentral.proteomexchange.org/cgi/GetDataset?ID=PXD037968).

Authors' contributions

YL performed the proteomic analysis and was a major contributor to writing the manuscript. FH analyzed the proteomic data and chose the target for further analysis. JD and XH collected samples for proteomic analysis and performed the western blotting. CZ and MW performed IHC and statistical analysis. DD conceived and designed the study. All authors read and approved the final version of the manuscript. DD and YL confirm the authenticity of all the raw data.

Ethics approval and consent to participate

The study was approved by Chongqing Medical University Ethics Committee and all patients provided written informed consent to participate.

Patient consent for publication

All patients involved in the study provided written informed consent for the publication of any data and accompanying images.

Competing interests

The authors declare that they have no competing interests.

References

1. Lim H, Devesa SS, Sosa JA, Check D and Kitahara CM: Trends in thyroid cancer incidence and mortality in the United States, 1974-2013. JAMA 317: 1338-1348, 2017.
2. Sung H, Ferlay J, Siegel RL, Laversanne M, Soerjomataram I, Jemal A and Bray F: Global cancer statistics 2020: GLOBOCAN estimates of incidence and mortality worldwide for 36 cancers in 185 countries. CA Cancer J Clin 71: 209-249, 2021.
3. Dal Maso L, Tavilla A, Pacini F, Serraino D, van Dijk BAC, Chirlaque MD, Capocaccia R, Larrañaga N, Colonna M, Agius D, *et al*: Survival of 86,690 patients with thyroid cancer: A population-based study in 29 European countries from EUROCARE-5. Eur J Cancer 77: 140-152, 2017.
4. Sparano C, Moog S, Hadoux J, Dupuy C, Al Ghuzlan A, Breuskin I, Guerlain J, Hartl D, Baudin E and Lamartina L: Strategies for radioiodine treatment: What's new. Cancers (Basel) 14: 3800, 2022.
5. Jin Y, Van Nostrand D, Cheng L, Liu M and Chen L: Radioiodine refractory differentiated thyroid cancer. Crit Rev Oncol Hematol 125: 111-120, 2018.
6. Mu ZZ, Zhang X and Lin YS: Identification of radioactive iodine refractory differentiated thyroid cancer. Chonnam Med J 55: 127, 2019.
7. Yu Q, Zhang X, Li L, Zhang C, Huang J and Huang W: Molecular basis and targeted therapies for radioiodine refractory thyroid cancer. Asia Pac J Clin Oncol 10: ajco.13836, 2022.
8. Jögi A, Vaapil M, Johansson M and Påhlman S: Cancer cell differentiation heterogeneity and aggressive behavior in solid tumors. Ups J Med Sci 117: 217-224, 2012.
9. Haugen BR, Alexander EK, Bible KC, Doherty GM, Mandel SJ, Nikiforov YE, Pacini F, Randolph GW, Sawka AM, Schlumberger M, *et al*: 2015 American thyroid association management guidelines for adult patients with thyroid nodules and differentiated thyroid cancer: The american thyroid association guidelines task force on thyroid nodules and differentiated thyroid cancer. Thyroid 26: 1-133, 2016.
10. Pirooznia N, Abdi K, Beiki D, Emami F, Arab SS, Sabzevari O and Soltani-Gooshkhaneh S: 177Lu-labeled cyclic RGD peptide as an imaging and targeted radionuclide therapeutic agent in non-small cell lung cancer: Biological evaluation and preclinical study. Bioorg Chem 102: 104100, 2020.
11. Schuchardt C, Zhang J, Kulkarni HR, Chen X, Müller D and Baum RP: Prostate-specific membrane antigen radioligand therapy using ^{177}Lu-PSMA I&T and ^{177}Lu-PSMA-617 in patients with metastatic castration-resistant prostate cancer: Comparison of safety, biodistribution, and dosimetry. J Nucl Med 63: 1199-1207, 2022.
12. Dai G, Levy O and Carrasco N: Cloning and characterization of the thyroid iodide transporter. Nature 379: 458-460, 1996.

13. Paladino S and Melillo RM: Editorial: Novel mechanism of radioactive iodine refractivity in thyroid cancer. J Natl Cancer Inst 109: 10.1093/jnci/djx106, 2017.
14. Luo G, Zhou J, Li G, Hu N, Xia X and Zhou H: Retracted: Ferruginol diterpenoid selectively inhibits human thyroid cancer growth by inducing mitochondrial dependent apoptosis, endogenous reactive oxygen species (ROS) production, mitochondrial membrane potential loss and suppression of mitogen-activated protein kinase (MAPK) and PI3K/AKT signaling pathways. Med Sci Monit 27: e932341, 2021.
15. Ban Z, He J, Tang Z, Zhang L and Xu Z: LRG-1 enhances the migration of thyroid carcinoma cells through promotion of the epithelial-mesenchymal transition by activating MAPK/p38 signaling. Oncol Rep 41: 3270-3280, 2019.
16. Li W, Qian C, Ma F, Liu M, Sun X, Liu X, Liu C, Chen Z, Ma W, Liu J, *et al*: MAPK/ERK-CBP-RFPL-3 mediates adipose-derived stem cell-induced tumor growth in breast cancer cells by activating telomerase reverse transcriptase expression. Stem Cells Int 2022: 8540535, 2022.
17. Ahmed AA, Farooqi MS, Habeebu SS, Gonzalez E, Flatt TG, Wilson AL and Barr FG: NanoString digital molecular profiling of protein and microrna in rhabdomyosarcoma. Cancers (Basel) 14: 522, 2022.
18. Wang Z, Zhang R, Liu F, Jiang P, Xu J, Cao H, Du X, Ma L, Lin F, Cheng L, *et al*: TMT-based quantitative proteomic analysis reveals proteomic changes involved in longevity. Prot Clin Appl 13: 1800024, 2019.
19. Kroksveen AC, Aasebø E, Vethe H, Van Pesch V, Franciotta D, Teunissen CE, Ulvik RJ, Vedeler C, Myhr KM, Barsnes H and Berven FS: Discovery and initial verification of differentially abundant proteins between multiple sclerosis patients and controls using iTRAQ and SID-SRM. J Proteomics 78: 312-325, 2013.
20. Li XJ, Pan HT, Chen JJ, Fu YB, Fang M, He GH, Zhang T, Ding HG, Yu B, Cheng Y, *et al*: Proteomics of uterosacral ligament connective tissue from women with and without pelvic organ prolapse. Prot Clin Appl 13: 1800086, 2019.
21. Zhou Y, Lih TM, Pan J, Höti N, Dong M, Cao L, Hu Y, Cho KC, Chen SY, Eguez RV, *et al*: Proteomic signatures of 16 major types of human cancer reveal universal and cancer-type-specific proteins for the identification of potential therapeutic targets. J Hematol Oncol 13: 170, 2020.
22. Liang JH, Lin Y, Ouyang T, Tang W, Huang Y, Ye W, Zhao JY, Wang ZN and Ma CC: Nuclear magnetic resonance-based metabolomics and metabolic pathway networks from patient-matched esophageal carcinoma, adjacent noncancerous tissues and urine. World J Gastroenterol 25: 3218-3230, 2019.
23. Fukui R, Saga R, Matsuya Y, Tomita K, Kuwahara Y, Ohuchi K, Sato T, Okumura K, Date H and Fukumoto M: Tumor radioresistance caused by radiation-induced changes of stem-like cell content and sub-lethal damage repair capability. Sci Rep 12: 1056, 2022.
24. Suwiwat S, Tungsinmunlong K and Siriaungkul S: Expression of CD44v6 and RCAS1 in uterine cervical carcinoma infected with human papillomavirus and its effect on cell proliferation and differentiation. Asian Pac J Cancer Prev 23: 2431-2439, 2022.
25. Cui Y, Liu Y, Mu L, Li Y and Wu G: Transcriptional expressions of ALDH1A1/B1 as independent indicators for the survival of thyroid cancer patients. Front Oncol 12: 821958, 2022.
26. Ravera S, Reyna-Neyra A, Ferrandino G, Amzel LM and Carrasco N: The Sodium/Iodide Symporter (NIS): Molecular physiology and preclinical and clinical applications. Annu Rev Physiol 79: 261-289, 2017.
27. Wang Z, Zhou Q, Li A, Huang W, Cai Z and Chen W: Extracellular matrix protein 1 (ECM1) is associated with carcinogenesis potential of human bladder cancer. Onco Targets Ther 12: 1423-1432, 2019.
28. Feng M, Dong N, Zhou X, Ma L and Xiang R: Myosin light chain 9 promotes the proliferation, invasion, migration and angiogenesis of colorectal cancer cells by binding to Yes-associated protein 1 and regulating Hippo signaling. Bioengineered 13: 96-106, 2022.
29. Luo D, Chen H, Lu P, Li X, Long M, Peng X, Huang M, Huang K, Lin S, Tan L, *et al*: CHI3L1 overexpression is associated with metastasis and is an indicator of poor prognosis in papillary thyroid carcinoma. Cancer Biomark 18: 273-284, 2017.
30. Dimitrova I, Shinkov A, Dodova R, Ivanova R, Kirilov G, Kyurkchiyan S, Kaneva R and Kovatcheva R: Increased gene expression of TIMP1 and CHI3L1 in fine-needle aspiration biopsy samples from papillary thyroid cancer as compared to benign nodules. Diagn Cytopathol 49: 1045-1051, 2021.
31. Moore RG, Blackman A, Miller MC, Robison K, DiSilvestro PA, Eklund EK, Strongin R and Messerlian G: Multiple biomarker algorithms to predict epithelial ovarian cancer in women with a pelvic mass: Can additional makers improve performance? Gynecol Oncol 154: 150-155, 2019.